

ARTICLE

# Analysis of the Geometry of Wear Tracks in Laser Deposited Stellite 6 Coatings

Alain Kusmoko<sup>1,2\*</sup> , Huijun Li<sup>1</sup> , Druce Dunne<sup>1</sup> 

<sup>1</sup>Department Material Engineering, University of Wollongong, Wollongong, NSW, 2522, Australia

<sup>2</sup>Department Mechanical Engineering, University of Muhammadiyah Surabaya, East Java, 60113, Indonesia

## ABSTRACT

A model has been developed to predict the wear groove geometry resulting from wear testing of Stellite 6 coatings on ferrous and nickel-based alloys produced by laser cladding with powers of 1 kW and 1.8 kW. Although the predictions of the model are close to the observed values, they differ in ways that can be accounted for by the incorrect assumption that only abrasive wear occurs. Abrasive wear is dominant, but there is also evidence that adhesive wear and plastic deformation occur and change the geometry and macrostructures of the wear tracks, particularly for the coatings on a Ni-based superalloy substrate. Significant differences were observed in wear track geometries and macrostructures for coatings on the substrates investigated and these differences correlate well with measured differences in the wear loss of the Stellite coatings.

**Keywords:** Geometry; Laser cladding; Stellite 6; Wear

## 1. Introduction

The sliding wear behaviour of Stellite 6 coated samples produced by laser cladding has been investigated and reported for six high strength alloy substrates in recent publications by the authors <sup>[1-7]</sup>.

The substrates consisted of medium carbon steel (MS), a nickel-based superalloy (NIS), martensitic stainless steel (MSS), austenitic stainless steel (ASS), 2.25% chromium creep resisting steel (P22) and 9% chromium creep resisting steel (P91). The laser powers were 1.0 and 1.8 kW and wear testing was

### \*CORRESPONDING AUTHOR:

Alain Kusmoko, Department Material Engineering, University of Wollongong, Wollongong, NSW, 2522, Australia; Department Mechanical Engineering, University of Muhammadiyah Surabaya, East Java, 60113, Indonesia; Email: akusmoko@uow.edu.au

### ARTICLE INFO

Received: 25 July 2023 | Revised: 7 November 2023 | Accepted: 21 December 2023 | Published Online: 27 January 2024

DOI: <https://doi.org/10.30564/jmmr.v7i1.5850>

### CITATION

Kusmoko, A., Li, H.J., Dunne, D., 2024. Analysis of the Geometry of Wear Tracks in Laser Deposited Stellite 6 Coatings. Journal of Metallic Material Research. 7(1): 14-21. DOI: <https://doi.org/10.30564/jmmr.v7i1.5850>

### COPYRIGHT

Copyright © 2024 by the author(s). Published by Bilingual Publishing Group. This is an open access article under the Creative Commons Attribution-NonCommercial 4.0 International (CC BY-NC 4.0) License (<https://creativecommons.org/licenses/by-nc/4.0/>).

carried out using 2 and 5 kg loads.

Work relevant to the present investigation has been reported by Bata [8] who addressed the microstructural characterisation of the new tool Ni-based alloy with high carbon and chromium content. Kusmoko et al. [9] have determined wear mode maps on induction hardened 4140 and carburised 8617H steel. Detailed analysis of laser material processing has been reported by Steen [10] and Lim et al. [11] have studied wear-rate transitions and their relationship to wear mechanisms.

In relation to the current work, **Table 1**, which is based on the results obtained and reported in reference [12], records wear loss data for the six substrates that were Stellite-coated using laser power of 1 and 1.8 kW. The table also lists the average coating hardness and the estimated carbon content of the coating. The data have been used to test a model developed to predict the wear groove geometry resulting from wear testing.

## 2. Materials and methods

The aim of this work was to produce a model to predict wear groove geometry resulting from wear testing of the six Stellite-coated substrates listed in the introduction. Each substrate was coated using

two laser powers (1.0 and 1.8 kW) and wear testing was carried out with loads of 2 and 5 kg.

A Beceri pin-on-plate (reciprocating mode) wear testing machine was used, with a 6 mm diameter tool steel ball as the “pin”. During operation, the ball remained stationary while the flat specimen was moved in a linear, forward and reverse sliding motion, under a prescribed set of conditions. The ball thus made contact in a straight-line path 20 mm long over the flat specimen, resulting in a path length of 40 mm/revolution. The test speed, number of cycles and test duration were held constant: 50 rpm, 10,000 cycles and 200 minutes. The Stellite 6 coatings were sectioned perpendicular to the coated surface using Struers Accutom-50 automatic cutting machine with an alumina cut-off-wheel. The hardness testing used Leco M-400-H1 hardness testing machine with a load of 300 g at interval of 0.05 mm across the coating thickness. Microstructural examination was conducted using a Leica DMRM optical microscope. In addition, surface worn samples were examined using a S440 scanning electron microscope.

The wear groove widths were measured using a micrometer magnifier and from photomicrographs obtained by means of a Nikon optical microscope.

**Table 1.** Wear loss, average coating hardness and estimated %C for each laser power and wear test load.

Substrate	Load (kg)	1.0 kW Laser Power			1.8 kW Laser Power		
		Wear loss (g)	Av. coating hardness (HV0.5)	Carbon (wt%)*	Wear loss (g)	Av. coating hardness (HV0.5)	Carbon (wt%)*
NIS	2	0.00995	450	0.665	0.02808	340	0.608
	5	0.06312	450	0.665	0.20760	340	0.608
ASS	2	0.00868	510	0.854	0.00996	440	0.795
	5	0.01984	510	0.854	0.03580	440	0.795
MS	2	0.0023	600	0.982	0.00302	510	0.944
	5	0.0090	600	0.982	0.01177	510	0.944
MSS	2	0.00280	550	0.897	0.00348	520	0.842
	5	0.01298	550	0.897	0.02228	520	0.842
P22	2	0.00270	600	0.961	0.00312	490	0.855
	5	0.00910	600	0.961	0.01558	490	0.855
P91	2	0.00488	560	0.882	0.00496	510	0.827
	5	0.01962	560	0.882	0.02736	510	0.827

\*Estimated carbon content based on coating dilution.

These data were compared with the predictions of a geometric model of the wear track. As well as groove width, the model provides an estimate of the maximum depth of the wear track. The model is based on the following assumptions:

- (a) The steel ball produces a wear track 20 mm long with a cross-sectional (C/S) area in the shape of a segment of a circle with 6 mm diameter;
- (b) The geometry of the ball does not change during the wear test;
- (c) There is no wear loss of the steel ball;
- (d) All of the measured mass loss arises from abrasive wear of the Stellite coating;
- (e) The microstructure and hardness of the material being wear tested are constant; and
- (f) The density of the Stellite coating is 8.44 g/cc<sup>[13]</sup>.

Assumption (c) was confirmed to be valid as the mass of the alloy steel ball was unchanged after wear testing, indicating that the measured wear loss for each wear test was associated only with the coated sample.

### 3. Results

Based on these assumptions, the volume of material removed can be calculated, as well as the C/S area of the wear track and its width. The coating depth was maintained at  $0.35 \pm 0.05$  mm for all samples<sup>[1-7]</sup>. The estimates of wear depth were compared to the actual coating depth to establish which, if any, wear tests resulted in penetration of the coating.

The two largest mass losses occurred for the Stellite coating on the nickel-based superalloy substrate: 0.2076 g for 1.8 kW laser power and 0.0631 g for 1.0 kW, both wear tested using a load of 5 kg (see **Table 1**). The next highest mass loss was 0.0358 g for the coating on the austenitic stainless steel substrate deposited at 1.8 kW and wear tested with a 5 kg load. All of the other mass losses were less than about 0.028 g.

The calculations conducted to arrive at the estimates of groove depth were carried out as follows. The assumed cross-section is a segment of a circle of 6 mm diameter as shown in **Figure 1**. The sector associated with the segment subtends an angle  $\theta$  (de-

grees) to the chord and boundaries of the segment. The area of the segment,  $A_{\text{seg}}$  (mm<sup>2</sup>), is given by the equation

$$A_{\text{seg}} = 0.5 r^2 (\theta\pi/180 - \sin\theta)$$

where  $r$  is the circle radius in mm and  $\theta$  is the sector angle in degrees corresponding to the completion of the wear test. The radius  $r$  in the present case is 3 mm and by using the angle  $\alpha$  which is half of the sector angle  $\theta$ , the groove depth  $d$  (mm) is given by  $3(1-\cos\alpha)$  and the groove width  $w$  (mm) is equal to  $6\sin\alpha$ .

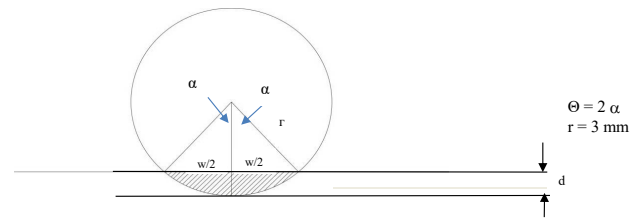


**Figure 1.** Schematic diagram showing cross-section of wear track profile which is a segment of a circle of radius,  $r$ . The depth of the wear track is  $d$  and its width is  $w$ . The segment area (hatched) is  $A_{\text{seg}}$ .

The travel length of the sample was 20 mm forward and 20 mm backwards. The travel length of 20 mm is the distance between the initial point contact of the ball with the sample and the point contact at the termination of the first 20 mm traverse. This fact is important as the geometric model predicts that the volume of coating material removed is  $20A_{\text{seg}}$  (mm<sup>3</sup>), whereas the actual volume will be slightly larger because of the end profile established by the wear ball. The volume removed can be converted into the mass removed by assuming that the density of the coating is 8.44 g/cm<sup>3</sup> ( $8.44 \times 10^{-3}$  g/mm<sup>3</sup>)<sup>[13]</sup>. As a result of the difference between assumed and actual wear track profiles, the mass loss predicted will be slightly lower than the actual amount.

The relationship between the sector angle  $\theta$  and the corresponding area of the segment is shown in **Figure 2**.

The volume of material removed at the completion of a wear test is  $20A_{\text{seg}}$  and the mass removed in grams is given by  $8.44 \times 10^{-3} \times 20A_{\text{seg}}$ . The estimated mass loss is plotted against the groove width and

the maximum groove depth in **Figure 3**.

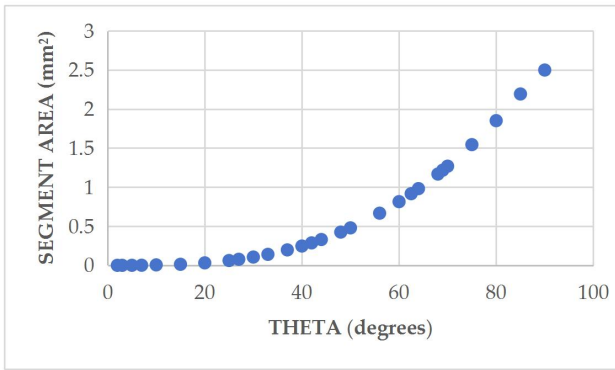


**Figure 2.** Segment area in mm<sup>2</sup> as a function of the sector angle  $\theta$  in degrees.

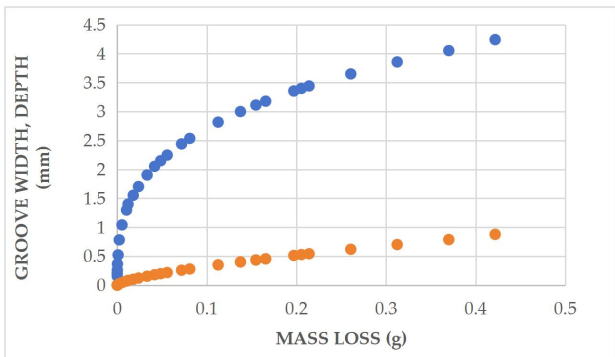


**Figure 3.** Predicted groove width and depth (mm) corresponding to the predicted wear mass loss (g).

The measured groove widths are plotted against measured mass loss in **Figure 4**. The trend of groove width with mass loss is similar to that predicted by the model in **Figure 3**, particularly for the more wear resistant samples with mass losses less than about 0.035 g (see **Table 1** and **Figure 5**).

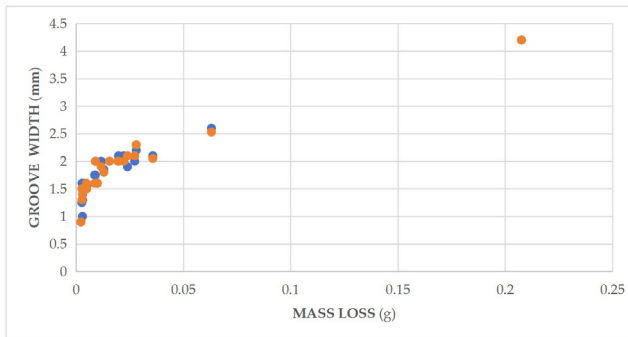


**Figure 4.** Measured groove widths (mm) plotted against measured mass losses in grams. Blue data points were obtained using a micrometer eyepiece and the red points by measurements from macrophotographs.

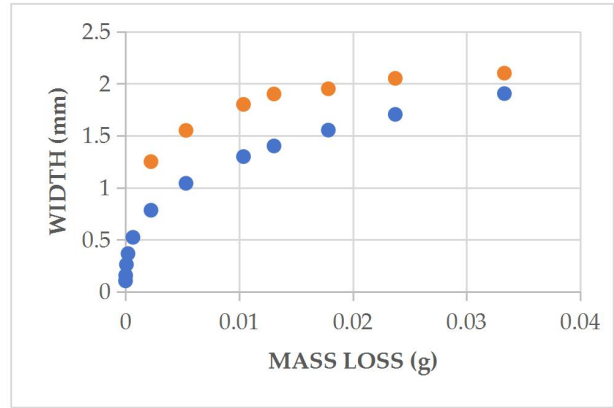


**Figure 5.** Plot of wear groove width and mass losses lower than about 0.035 g. Blue data points are predicted values; and the red points are average measured values selected from that data points shown in **Figure 4**.

Although **Figure 5** shows that the mass loss-width relationship is similar for both the measured and predicted results, the measured widths for a given mass loss were typically about 0.5 mm larger than those predicted. Possible reasons for this difference are discussed in the following section.

## 4. Discussion

The two outlier values for measured groove width are for the NIS substrate: 4.2 mm for the condition 1.8 kW/5 kg and 3.0 mm for 1 kW/5 kg (**Table 1**). If these two measured widths are applied to the upper curve for the geometric model predictions shown in **Figure 3**, the predicted mass losses are about double the measured values of 0.207 g and 0.063 g for 1.5 kW and 1 kW, respectively (see **Figure 4**). According to the model (**Figure 3**), these two measured mass losses correspond to groove widths of about 3.45 mm and 2.25 mm, about 80% of the measured widths. The corresponding groove depths are predicted to be 0.55 mm (1.8 kW) and 0.30 mm (1 kW), exceeding the coating depth of 0.35 mm for the higher estimate and close to the coating-substrate border for the other. Therefore, these wear tests could have resulted in penetration or near-penetration of the coating and wear and/or deformation of the underlying substrate HAZ. In all other cases, the wear would have been well confined to the coating.

This hypothesis was tested by measuring the depth of the wear track using the calibrated fine focus control of a Nikon optical microscope. The results for 5 kg wear tests for NIS were 0.30 mm and 0.51 mm for laser powers of 1 and 1.8 kW, respectively. These values are almost identical with the predicted depths and are higher than or close to the average coating thickness of 0.35 mm.

Overall, the model is consistent with the measured groove depths but not the groove widths. This difference is most likely to be due to plastic deformation at the groove edges that results in increases in groove width. In effect, the steel ball acts like a dynamic hardness test indenter and produces plastic flow as well as removal of material.

It is therefore likely that the measured mass losses are lower than those predicted because the wear test, in addition to abrasive wear can result in plastic deformation of the coating, without mass loss. This effect could be particularly significant along the contact edges with the steel ball, thereby increasing the apparent groove width without mass loss. Displacement of material at the edges of hardness indentation tests is a well-known phenomenon and in this case of wear testing the indenter (the loaded ball) is impressed on the coating for 10,000 cycles of sliding contact. As a result, the measured groove widths could be significantly higher than those predicted by the model which assumes that only abrasive wear occurs, assumption (d).

It is also possible that elastic strain occurs in the ball which results in flattening of the contact surface of the ball with the test plate. If this effect does occur, it would invalidate model assumptions (a) and (b). Although the initial contact of the ball with the test plate will be a point contact, it will become a contact arc that lengthens as the wear groove develops and line contact becomes areal contact. Therefore, the contact stress would be expected to decrease continuously during wear testing. A rough calculation of the instantaneous stress on the ball can be made for a sector angle of  $30^\circ$ . The arc length

of contact will be 1.57 mm and assuming a contact width of 0.1 mm, the contact area is  $0.157 \text{ mm}^2$ . The load of 5 kg will result in a contact stress of about 318 MPa and an elastic strain of  $0.66 \times 10^{-3}$  (taking Young's Modulus to be 210 GPa). Elastic strain over the 6 mm diameter ball will be about  $4 \times 10^{-3}$  mm which is not nearly large enough to change the ball contact profile in such a way that it could account for the apparent width spread.

Another issue is the use of a reported density for undiluted Stellite of a composition similar to that specified by the supplier for the alloy used in this work. Dilution by the elements of the substrate alloys is expected to lower this density and therefore, reduce the predicted mass loss. Moreover, the extent of coating dilution varied significantly with the identity of the substrate alloy, with the minimum being about 5% for the mild steel substrate for coating at a laser power of 1 kW, and the maximum being about 40% for the coating deposited on the Ni-based superalloy substrate at 1.8 kW<sup>[1-7]</sup>. Therefore, the density of the diluted coating would have varied with the identity of the substrate, as well as the laser deposition power which affects the extent of dilution. Assumption (f) is invalid as the actual coating density would be lower than 8.44 g/cc by an amount that differs for each substrate and for each of the two deposition powers. The maximum difference will be for the coating deposited at 1.8 kW on the Ni-based substrate, which showed 40% dilution<sup>[1-7]</sup>. The Ni-based substrate was the alloy IN 718 which has a density of 8.14 g/cc. A simple rule of mixtures calculation indicates a density of the diluted coating of 8.22 g/cc. Re-calculation of predicted mass loss only produces a decrease in mass that is too small to reconcile the difference between predicted and measured mass loss.

Macrographs of wear tracks are shown in **Figures 6 and 7** for Stellite-coated mild steel and Ni superalloy substrates, wear tested using loads of 2 and 5 kg. The wear grooves for these two cases are associated with the lowest and highest mass losses.

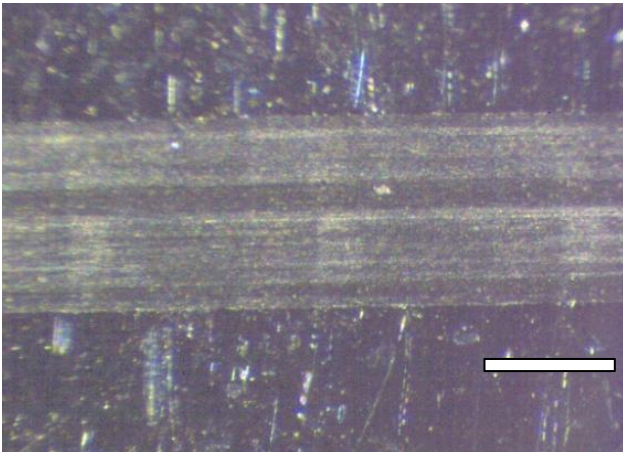


**Figure 6.** Wear grooves on Stellite-coated mild steel substrate with 1 kW laser power, wear tested using loads of 2 and 5 kg. The bar represents 2 mm.

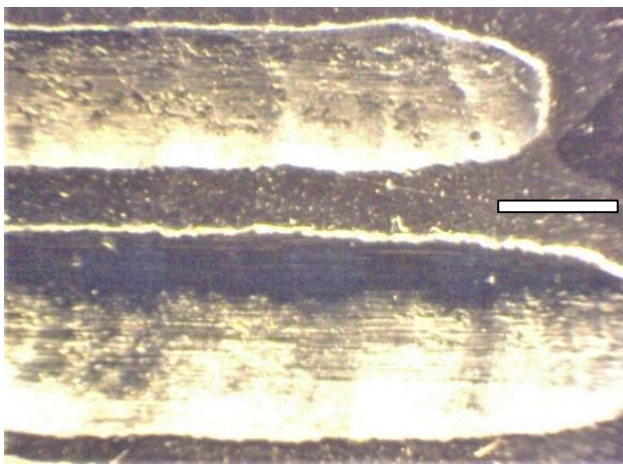


**Figure 7.** Wear grooves on Stellite-coated Ni alloy substrate using 1.8 kW laser power, wear tested with loads of 2 and 5 kg. The bar represents 2 mm.

Scanning electron microscopy (SEM) showed variable morphologies for the wear tracks depending on the substrate material. The wear grooves for the worn surface of NIS and MS, coated with 1.8 kJ laser power and tested at a load of 5 kg, are shown in **Figures 8 and 9**, respectively.

The mass losses in these two cases were 0.01177 g for the MS substrate and 0.20760 g for the NIS substrate, differing by a factor of about 20. The wear morphologies were also significantly different, as the MS sample showed a relatively smoothly worn surface whereas the NIS sample exhibited a much rougher surface with evidence of considerable plastic flow and exfoliation of wear particles. Further, the wear track appeared macroscopically

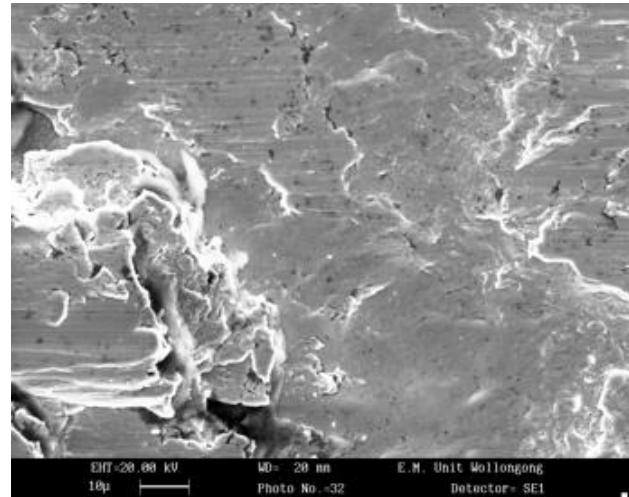


**Figure 8.** SEM micrograph of worn surface of Stellite deposited at 1.8 kJ on the Ni-based alloy substrate (NIS), tested with a load of 5 kg.

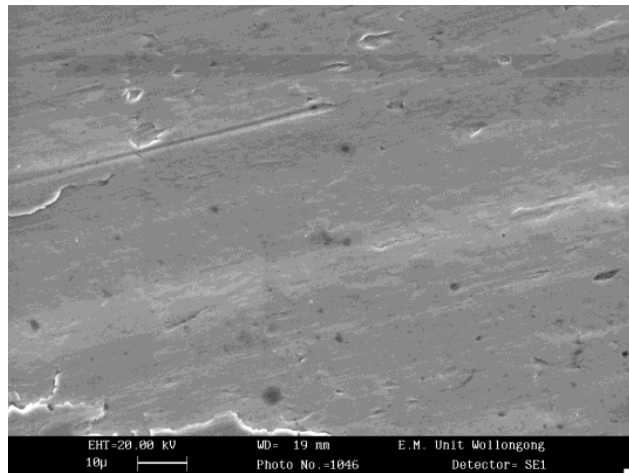


**Figure 9.** SEM micrograph of worn surface of Stellite deposited at 1.8 kJ on mild steel substrate (MS), tested with a load of 5 kg.

to be undulating (see **Figure 7**), suggesting that the motion of the test sample against the fixed ball was chattered rather than smooth. A possible reason could be a component of adhesive wear in addition to sliding wear. **Figures 7 and 9** are also consistent with the wear test extending below the Stellite coating into the substrate heat affected zone (HAZ) and possibly into the unaffected substrate material. Full strengthening of this Ni-based superalloy is developed by specific ageing heat treatments to produce fine coherent intermetallic precipitates. In contrast, the heat treatment by laser deposition is uncontrolled and the alloy would be expected to have a solution treated austenitic structure in the

HAZ close to the interface with the deposited coating alloy. The temperature gradient due to deposition produces a microstructural gradient in the HAZ with solution treated austenite adjacent to the coating and, with depth, austenite containing intermetallics with a range of volume fractions and size distributions depending on the local thermal history. The measured hardness of the substrate was 200 HV and the average HAZ hardness was 240 HV <sup>[2,3]</sup>. These hardness values are low enough for the substrate material underlying the coating to deform plastically under the wear loading conditions. Moreover, the Stellite coating itself had the lowest hardness of all of the substrates (see **Table 1**), resulting in the highest wear losses and substantial plastic deformation and tearing, in addition to abrasive wear (**Figures 7 and 8**). In contrast, the much higher surface hardness on the mild steel coated sample is likely to have resulted in formation of a brittle oxide layer due to the high flash temperature at contacting asperities under the sliding wear conditions. Oxide fragments break away to produce wear debris but the oxide is continuously replenished and limits metal-to-metal contact <sup>[11]</sup>. Therefore, the abrasive wear loss for the coated mild steel substrate was very low.

## 5. Conclusions

The proposed model for the wear groove geometry is broadly consistent with the observed values, but it differs in a way that can be accounted for by the incorrect assumption that only abrasive wear occurs. Although abrasive wear is dominant, there is evidence that adhesive wear and plastic deformation also occur and change the geometry and macrostructures of the wear tracks, particularly for the coatings on the Ni-based superalloy substrate. Differences in the wear track geometries and macrostructures correlate well with differences in wear resistance of the Stellite coatings on the two alloy substrates that were examined metallographically.

## Conflict of Interest

There is no conflict of interest.

## Author Contributions

All authors have equal contributions.

## References

- [1] Kusmoko, A., Dunne, D., Li, H., 2017. Dilution and C content estimation of Stellite 6 fabricated on a 1050 steel substrate by laser cladding. *Solid State Phenomena*. 263, 131–136. DOI: <https://doi.org/10.4028/www.scientific.net/SSP.263.131>
- [2] Kusmoko, A., Dunne, D., Li, H., 2014. Study of laser cladding of Stellite 6 on nickel superalloy substrate with two different energy inputs. *Advanced Materials Research*. 896, 600–604. DOI: <https://doi.org/10.4028/www.scientific.net/AMR.896.600>
- [3] Kusmoko, A., Dunne, D.P., Li, H., 2013. Deposition of Stellite 6 on nickel superalloy and mild steel substrates with laser cladding. *Advanced Materials Manufacturing and Characterisation*. 3, 469–473. DOI: <http://dx.doi.org/10.11127/ijammc.2013.07.01>
- [4] Kusmoko, A., Dunne, D., Li, H., 2014. Effect of two different energy inputs for laser cladding of Stellite 6 on P91 and P22 steel substrates. *Procedia Materials Science*. 6, 26–36. DOI: <https://doi.org/10.1016/j.mspro.2014.07.005>
- [5] Kusmoko, A., Dunne, D., Li, H., 2015. Effect of heat input on Stellite 6 coatings on a medium carbon steel substrate by laser cladding. *Materials Today: Proceedings*. 2(4–5), 1747–1754. DOI: <https://doi.org/10.1016/j.matpr.2015.07.010>
- [6] Kusmoko, A., Dunne, D.P., Li, H., 2016. Measuring dilution and wear for laser cladding of Stellite 6 produced on a P91 steel substrate using two different heat inputs. *Matec Web of Conferences*. 70, 01001. DOI: <http://dx.doi.org/10.1051/mateconf/20167001001>
- [7] Kusmoko, A., Dunne, D.P., Dahar, R., Li, H.,

2014. Surface treatment evaluation of induction hardened and tempered 1045 steel. *Current Engineering and Technology*. 4, 1236–1239.
- [8] Bała, P., 2010. Microstructural characterization of the new tool Ni-based alloy with high carbon and chromium content. *Archives of Metallurgy and Materials*. 55, 1053–1059.
- [9] Kusmoko, A., Crosky, A., 2013. Wear mode map evaluation of induction hardened 4140 and carburised 8617H steels on 1040 steel. *Advanced Materials Manufacturing and Characterisation*. 3, 474–479.  
DOI: <http://dx.doi.org/10.11127/ijammc.2013.07.02>
- [10] Steen, W., 2003. *Laser material processing*. Springer: London.
- [11] Lim, S.C., Ashby, M.F., Brunton, J.H., 1987. Wear-rate transitions and their relationship to wear mechanisms. *Acta Metallurgica*. 35(6), 1343–1348.  
DOI: [https://doi.org/10.1016/0001-6160\(87\)90016-2](https://doi.org/10.1016/0001-6160(87)90016-2)
- [12] Kusmoko, A., 2016. Effect of laser power and steel and nickel-based alloy substrates on hardness and wear resistance of laser-deposited alloys stellite coatings [Ph.D. thesis]. Wollongong: University of Wollongong.
- [13] *Stellite Alloys—Chemical Composition, Mechanical Properties and Common Applications* [Internet]. AZO Materials. Available from: <https://www.azom.com>